Estimation of Input Pulse Locations From the Response of an All-Pole Transfer System Using Tapered Rank Reduction

Hiroshi Kanai, *Associate Member, IEEE*, and Ken'iti Kido, *Member, IEEE*

***Abstract*—When a multipulse input time series is estimated from the response of a transfer system, it is necessary to remove characteristics of the transfer system from the response signal before applying the previously proposed method for estimating the input pulse locations. When the ordinary rank reduction is used to remove the characteristics of the transfer system and to estimate the multipulse input time series, the nonsignificant singular values are sharply cut off by low-order truncation if the system Q (quality factor) is high, and then a large ripple occurs around each pulse location. In order to avoid these difficulties, we propose a new method where the multipulse time series is estimated by a rank reduction using a *tapering* window in order to suppress the ripple due to the low-order sharp truncation, and then by applying the pole-estimation method to the inverse Fourier transform of the resultant time series, the pulse locations are accurately estimated. By using the pulse locations as the initial estimates, the maximum likelihood estimates of the pulse locations are obtained. From simulation experiments, these principles are confirmed.**

I. Introduction

LET $x(n)$, $n = 0, 1, \cdots, N-1$ be a multipulse input time series, which has N_p pulses, represented by

$$x(n) = \sum_{i=1}^{N_p} d_i \cdot \delta(n - \tau_i) \tag{1}$$

where

$$\delta(n) = \begin{cases} 1, & \text{if } n = 0; \\ 0, & \text{otherwise} \end{cases}$$

d_i and τ_i, $(0 \le \tau_1 < \tau_2 < \cdots < \tau_{N_p} < N)$ are the unknown amplitude and the unknown location of ith pulse, respectively. Suppose the response of a transfer system to the multipulse input time series $x(n)$ is received by a sensor in the form

$$y(n) = h(n) + w(n) \qquad (n = 0, 1, \cdots, N-1) \tag{2}$$

where $w(n)$ is the additive noise component assumed to be independent of the input signal $x(n)$, $h(n)$ is a response of an Mth order all-pole model $1/A(z) = 1/\Sigma_{m=1}^{M} a_m z^{-m}$ to $x(n)$ as

$$h(n) = -\sum_{m=1}^{M} a_m \cdot h(n-m) + x(n)$$

Manuscript received June 14, 1988; revised February 2, 1990.

H. Kanai is with the Department of Electrical Engineering, Faculty of Engineering, Tohoku University, Sendai 980, Japan.

K. Kido is with the Research Center for Applied Information Sciences, Tohoku University, Sendai 980, Japan.

IEEE Log Number 9040370.

M is the assumed order of the all-pole model, and $\{a_m\}$, $m = 0, 1, \cdots, M$ are known linear predictive coefficients ($a_0 = 1$). The problem is to estimate the time delays $\{\tau_i\}$ and the input time series $\{x(n)\}$ from a short-length (N-point) record of $\{y(n)\}$. This is the same problem as the analysis-by-synthesis of a vowel voice [1], [2] or a multipath time delay estimation [3]–[6], which arises in various fields such as geophysics, radar, and underwater acoustics. A performance limit of the multipath delay estimation has been also investigated in several papers [7]–[9]. In other papers [10]–[13], both the input signal $x(n)$ and the output signal $y(n)$ are used to estimate a multipath time delay. Since the number of spectrum zeros produced by the multipulse time series depends not on the number of the pulses but on the interval of the pulses, the promising pole-zero estimation approaches [14]–[17] cannot be applied to the estimation of the multipulse time series from the response signal $y(n)$.

One of the key questions to be addressed in this paper is how to estimate the multipulse input time series $\{x(n)\}$ in the case where the signal-to-noise ratio (SNR) is low and the system Q (quality factor) is high. That is, the transfer system has at least one pole which is close to the unit circle in the z plane.

A traditional way to estimate the time delays is to use autocorrelation of the output signal $y(n)$ [5], [10], [18], [19]. The delay differences can be estimated from the corresponding peaks of the resultant correlogram as long as the time delay differences are greater than the length of the signal autocorrelation [8]. If the system Q is high, however, the peaks due to the characteristics of the transfer system are much larger than the peaks due to the time delay differences. Thus, it is difficult to estimate the time delays from the resulting correlogram of the output signal $y(n)$ without removing the characteristics of the transfer system.

If the characteristics of the transfer system are removed, this problem is analogous to the estimation of the frequencies of the sinusoids in noise. Some methods for estimating time delays of a finite length output signal $y(n)$ in additive white noise were proposed [12]–[14], [19] as a direct implementation of maximum likelihood (ML). If the number N_p of pulses is large, this nonlinear least square search becomes computationally unattractive for practical implementations, especially in the cases where the reasonable initial estimates cannot be used.

Other methods which minimize the computational effort have been proposed such as so-called high-resolution methods [6], [11], [20]–[22]. One such method, called modified forward-backward linear prediction (MFBLP) [23]–[26], proposed by

1053-587X/91/0100-0148$01.00 © 1991 IEEE

Kumaresan and Tufts, is especially promising if the transfer system has a flat power spectrum.

If the system Q is high, it is necessary to remove the characteristics of the transfer system from the output signal $y(n)$ before applying the above high-resolution method. In such cases, however, frequency components other than at the resonant frequencies are easily affected by additive noise. Then an ordinary inverse filtering [1] cannot whiten the output signal because the frequency components which are contaminated by noise are emphasized by multiplying the inverse characteristics $A(z)$ of the transfer system. The similar whitening procedure in frequency domain is used in [20].

The rank reduction technique [27] can be applied for removing the transfer characteristics from the output signal $y(n)$ by truncating nonsignificant singular values of the transfer characteristics. In this case, it is important to determine the optimum truncation order [28], and a constructive procedure for selecting rank was addressed by Scharf and Tuft [29]. If the system Q is high, only a few singular values are significant, and then large ripples are caused around each pulse location due to the low-order sharp truncation.

We propose a new rank reduction method using a tapering window in order to suppress the ripples and clarify each pulse location in the resultant multipulse time series. In [30], we proposed a method to estimate multipulse time series based on the singular-value decomposition (SVD) using the tapering window. It presents a simple example showing that the ripples are suppressed by the tapering window. Its principle was, however, not described sufficiently and the improvement in the estimation accuracy of each pulse location was not evaluated. The present paper presents the principle of the tapered rank reduction in detail, and by combining it with the MFBLP method and an ML approach, we propose a new method to estimate the multipulse time series and each pulse location. These principles of this three-stage procedure are confirmed experimentally by comparing the estimates with those obtained from the rank reduction without using the tapering window. Throughout the paper, we assume that characteristics of the transfer system and the number N_p of pulses are known. Estimation of the order M of the transfer system and the number N_p of the pulses has been investigated in several papers (see [31], and its references). We also assume that the additive noise components $w(n)$ is white Gaussian.

II. Formulation of Minimum-Norm Least Square Estimation

Since the location of each pulse cannot be previously determined, it is necessary to assume that the N-length multipulse time series $x(n)$ of (1) has N pulses ($N_p = N$) such as

$$x(n) = \sum_{i=0}^{N-1} d_i \cdot \delta(n - i). \tag{3}$$

Using vectors $\boldsymbol{y} = [y(0), y(1), \cdots, y(N-1)]^T$, $\boldsymbol{h} = [h(0), h(1), \cdots, h(N-1)]^T$, $\boldsymbol{x} = [x(0), x(1), \cdots, x(N-1)]^T$, and $\boldsymbol{w} = [w(0), w(1), \cdots, w(N-1)]^T$, where the superscript T denotes the matrix transpose, $y(n)$ of (2) is given by

$$\begin{aligned} \boldsymbol{y} &= \boldsymbol{h} + \boldsymbol{w} \\ &= H\boldsymbol{x} + \boldsymbol{w} \end{aligned} \tag{4}$$

where H is the $N \times N$ lower triangular Toeplitz matrix such that

$$H = \begin{pmatrix} h_0(0) & 0 & \cdots & 0 \\ h_0(1) & h_0(0) & \cdots & 0 \\ \vdots & \vdots & \ddots & \vdots \\ h_0(N-2) & h_0(N-3) & \cdots & 0 \\ h_0(N-1) & h_0(N-2) & \cdots & h_0(0) \end{pmatrix}, \quad (h_0(0) = 1)$$

and $h_0(n)$, $(n = 0, 1, \cdots, N-1)$ is the response of the transfer system to a unit impulse $\delta(n)$. By minimizing the power of noise $\boldsymbol{w}$, the linear least square solution of $\boldsymbol{x}$, denoted by $\hat{\boldsymbol{x}}$, is obtained by

$$\hat{\boldsymbol{x}} = (H^TH)^{-1}H^T\boldsymbol{y}. \tag{5}$$

Let A be an $N \times N$ lower triangular Toeplitz matrix defined by using the linear predictive coefficients $\{a_m\}$ such that

$$A = \begin{bmatrix} a_0 & 0 & \cdots & \cdots & \cdots & \cdots & 0 \\ a_1 & a_0 & \ddots & & & & 0 \\ \vdots & \ddots & \ddots & \ddots & & & \vdots \\ a_M & \ddots & \ddots & \ddots & \ddots & & \vdots \\ 0 & a_M & \ddots & \ddots & \ddots & \ddots & \vdots \\ \vdots & \ddots & \ddots & \ddots & \ddots & a_0 & 0 \\ 0 & \cdots & 0 & a_M & \cdots & a_1 & a_0 \end{bmatrix}$$

where $a_0 = 1$. Since $AH = I$, where I is the $N \times N$ unit matrix, and $\det A = \det H = 1$, the solution $\hat{\boldsymbol{x}}$ of (5) is equal to $A\boldsymbol{y}$. By substituting $\boldsymbol{y}$ of (4)

$$\begin{aligned} \hat{\boldsymbol{x}} &= A\boldsymbol{y} \\ &= \boldsymbol{x} + A\boldsymbol{w}. \end{aligned} \tag{6}$$

That is, the resultant signal $\hat{\boldsymbol{x}}$ is the sum of the true components of the input time series $\boldsymbol{x}$ and the noise components $A\boldsymbol{w}$, which is caused by the whitening procedure. Though the determinant of H or A is always equal to unity, the ratio of the minimum to the maximum singular values is very small if the system Q is high. In such cases, the power of the second term $A\boldsymbol{w}$, which is represented by an all-zero process, is much larger than that of the first term $\boldsymbol{x}$.

In order to avoid difficulties in estimating a multipulse time series in low SNR cases, the minimum-norm solution to the above linear least square problem is obtained using the rank reduction technique [32] as follows: Let $\{\psi_i\}$, $i = 1, 2, \cdots, N$ be nonzero singular values of H. Then the matrix H is represented in the general form

$$H = Q_1 \Psi Q_2^T \tag{7}$$

where Q_1 and Q_2 are $N \times N$ unitary matrices which are composed of the orthonormal eigenvectors of HH^T and H^TH, respectively, and the matrix Ψ has ψ_i in the i, i position ($1 \le i \le N$) and zeros elsewhere such that $\Psi = \text{diag}\,[\psi_1, \psi_2, \cdots, \psi_N]$, where $\psi_1 \ge \psi_2 \ge \cdots \ge \psi_N > 0$. Suppose the singular values $\{\psi_i\}$, $i = R+1, R+2, \cdots, N$ are nonsignificant and that the rank of H is approximately equal to R. Then the minimum-norm linear least square estimate $\hat{\boldsymbol{x}}$ of (5) is obtained by

$$\hat{\boldsymbol{x}} = Q_2 \Psi_R^{-1} Q_1^T \boldsymbol{y} \tag{8}$$

where $\Psi_R^{-1} \overset{\text{def}}{=} \text{diag}\,[1/\psi_1, \cdots, 1/\psi_R, 0, \cdots, 0]$. The physical meaning of the estimate $\hat{x}$ is given below. The $N \times N$ Toeplitz matrix H, when multiplied by the $N \times N$ order reversal matrix J, becomes a symmetric matrix JH, which is broken down using the eigen value $\{\sigma_i\}$ of the matrix JH as [32]

$$JH = U\Sigma U^T \tag{9a}$$

where

$$J = \begin{pmatrix} 0 & 0 & \cdots & 0 & 1 \\ 0 & 0 & \cdots & 1 & 0 \\ \cdots & \cdots & \cdots & \cdots & 0 \\ 0 & 1 & \cdots & 0 & 0 \\ 1 & 0 & \cdots & 0 & 0 \end{pmatrix}$$

$\Sigma \overset{\text{def}}{=} \text{diag}\,[\sigma_1, \sigma_2, \cdots, \sigma_N]$ is a $N \times N$ diagonal matrix and U is the unitary matrix composed of the eigenvectors $\{u_i\}$ of H. By neglecting nonsignificant eigenvalues $\{\sigma_i\}$, $i = R + 1, \cdots, N$, JH is approximately given by

$$JH \simeq U\Sigma_R U^T \tag{9b}$$

where $\Sigma_R = \text{diag}\,[\sigma_1, \sigma_2, \cdots, \sigma_R, 0, \cdots, 0]$. Since $J^2 = J^TJ = I$, then the term $(H^TH)^{-1}H^T$ of (5) is approximately equal to $U\Sigma_R^{-1}U^TJ$, where Σ_R^{-1} is defined by $\text{diag}\,[1/\sigma_1, 1/\sigma_2, \cdots, 1/\sigma_R, 0, \cdots, 0]$. Thus, the minimum-norm least square estimate $\hat{x}$ of x is given by

$$\hat{x} = U\Sigma_R^{-1}U^TJy. \tag{10}$$

Equation (10) is rewritten by use of (4) and (9b) such that

$$\begin{aligned} \hat{x} &= U\Sigma_R^{-1}U^TJ(JU\Sigma_RU^Tx + w) \\ &= (U^T)^{-1}\Delta_RU^Tx + (U^T)^{-1}\Sigma_R^{-1}U^Tw' \end{aligned} \tag{11}$$

where

$$\begin{aligned} \Delta_R &= \Sigma_R^{-1}\Sigma \\ &= \text{diag}\,[\overbrace{1, \cdots, 1}^{R}, \overbrace{0, \cdots, 0}^{N-R}] \end{aligned}$$

and $w' = Jw$ is the time-reversed noise signal. That is, $w'(n) \overset{\text{def}}{=} w(N - n - 1)$. The first term $(U^T)^{-1}\Delta_RU^T$ of (11) represents a low-order-passing filter as illustrated in Fig. 1(a). If each column eigenvector u_i of U is the orthonormal basic vector used in the N-point discrete Fourier transform, the term $(U^T)^{-1}\Delta_RU^T$ indicates the ordinary bandpass filter. The second term $(U^T)^{-1}\Sigma_R^{-1}U^T$ of (11) denotes a high-order-emphasis filter. By truncating the order greater than R, the noise term is suppressed and the stable estimate $\hat{x}$ of the multipulse time series is obtained even in low SNR cases. However, the sharp and low-order truncation of (10) leads to a large ripple around each pulse location in a similar manner as the well-known Gibbs phenomenon [33].

III. Rank Reduction Using a Tapering Window

In order to suppress the ripple and clarify the location of each excitation pulse, we propose a new rank reduction method using a tapering window $\lambda_1, \lambda_2, \cdots, \lambda_N$. Let Λ be a $N \times N$ diagonal matrix, of which diagonal components are composed of the tapering window as $\Lambda \overset{\text{def}}{=} \text{diag}\,[\lambda_1, \lambda_2, \cdots, \lambda_N]$. When a tapering window is used in the rank reduction, the minimum-norm least square estimate $\hat{x}$ of the multipulse input time signal is

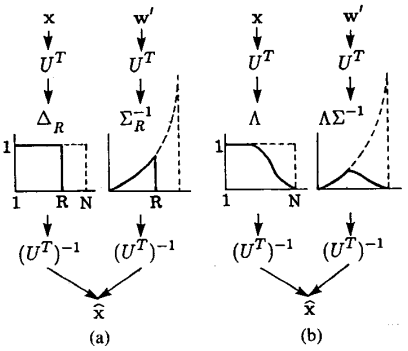

Fig. 1. The principle of the method for estimating the multipulse time series $\hat{x}$ using the low-order-passing filter formed by (a) the ordinary rank reduction and (b) the tapered rank reduction.

represented using the matrix $\Lambda\Psi^{-1}$ instead of $\Psi_R^{-1} = \Delta_R\Psi^{-1}$ of (8) or the matrix $\Lambda\Sigma^{-1}$ instead of $\Sigma_R^{-1} = \Delta_R\Sigma^{-1}$ of (10) as

$$\hat{x} = Q_2\Lambda\Psi^{-1}Q_1^Ty \tag{12}$$

or

$$\hat{x} = U\Lambda\Sigma^{-1}U^TJy. \tag{13}$$

In (12) or (13), nonsignificant singular values are neglected by using a tapered window $\lambda_1, \lambda_2, \cdots, \lambda_N$. By using (4) and (9a) and the property $U = (U^T)^{-1}$, (13) is rewritten as

$$\hat{x} = (U^T)^{-1}\Lambda U^Tx + (U^T)^{-1}\Lambda\Sigma^{-1}U^Tw'. \tag{14}$$

(See Fig. 1(b)). The tapering window has the effect of suppressing the ripple as described below. Let vector

$$d_i = [\overbrace{0, \cdots, 0}^{i-1}, 1, \overbrace{0, \cdots, 0}^{N-i}]^T$$

denote an N-length input time sequence having a unit pulse at time i. When d_i is used instead of x in (14), the first term becomes $(U^T)^{-1}\Lambda U^Td_i$. By letting $[u_{1i}, u_{2i}, \cdots, u_{Ni}]^T$ be the component of the ith column vector u_i of U, the estimated time series in the case of SNR $= \infty$, denoted by $\hat{d}_{i\infty}$, is represented as

$$\begin{aligned} \hat{d}_{i\infty} &= (U^T)^{-1}\Lambda U^Td_i \\ &= \begin{pmatrix} u_{11} & u_{12} & \cdots & u_{1N} \\ u_{21} & \ddots & \ddots & \vdots \\ \vdots & \ddots & \ddots & \vdots \\ u_{N1} & \cdots & \cdots & u_{NN} \end{pmatrix} \begin{pmatrix} \lambda_1 & 0 & \cdots & 0 \\ 0 & \lambda_2 & \ddots & \vdots \\ \vdots & \ddots & \ddots & 0 \\ 0 & \cdots & 0 & \lambda_N \end{pmatrix} \\ &\quad \cdot \begin{pmatrix} u_{i1} \\ u_{i2} \\ \vdots \\ u_{iN} \end{pmatrix} \\ &= \begin{pmatrix} \sum_{j=1}^{N} \lambda_j u_{ij} u_{1j} \\ \cdots \\ \sum_{j=1}^{N} \lambda_j u_{ij} u_{Nj} \end{pmatrix} \\ &= d_i - \sum_{j=1}^{N} (1 - \lambda_j) u_{ij} u_j \end{aligned}$$

where the property $\Sigma_{k=1}^{N} u_{ik}u_{jk} = \delta_{ij}$ is used. In ordinary inverse filtering, each λ_j, ($j = 1, 2, \cdots, N$) is equal to 1 and then $\hat{d}_{i\infty}$ become d_i. In the case of the rank reduction of (10), however, Λ is denoted by

$$\text{diag}\,[\overbrace{1, \cdots, 1}^{R}, \overbrace{0, \cdots, 0}^{N-R}]$$

and $\hat{d}_{i\infty}$ becomes $d_i - \Sigma_{j=R+1}^{N} u_{ij}u_j$, of which the second term indicates the ripple around the unit impulse due to the low-order sharp truncation. The power $\|\hat{d}_{i\infty}\|^2$ of $\hat{d}_{i\infty}$ estimated by using the tapering window $\lambda_1, \lambda_2, \cdots, \lambda_N$ is given by

$$\|\hat{d}_{i\infty}\|^2 = \sum_{j=1}^{N} \lambda_j^2 u_{ij}^2.$$

The estimated amplitude $\hat{d}_{i\infty}$ of the ith impulse is equal to $\Sigma_{j=1}^{N} \lambda_j u_{ij}^2$. On the other hand, the noise power of the second term of (14), denoted by $\|\hat{w}\|^2$, is

$$E[\|\hat{w}\|^2] = E[\|U\Delta\Sigma^{-1}U^T w'\|^2] = \sigma_w^2 \sum_{j=1}^{N} \left(\frac{\lambda_j}{\sigma_j}\right)^2$$

where σ_w^2 is the power of additive noise. Assuming that the noise component is independent of the input time series, the ratio of the square of the estimated amplitude $\hat{d}_{i\infty}$ of the ith pulse to the total power of the estimated input time series and the noise term is represented by

$$\nu(d_i) = \frac{\|\hat{d}_{i\infty}\|^2}{\|\hat{d}_{i\infty}\|^2 + \|\hat{w}\|^2} = \frac{\left\|\sum_{j=1}^{N} \lambda_j u_{ij}^2\right\|^2}{\sum_{j=1}^{N} \lambda_j^2 u_{ij}^2 + \sigma_w^2 \sum_{j=1}^{N} (\lambda_j/\sigma_j)^2}. \quad (15)$$

Take the simplest example of a signal length of $N = 3$, and a nonsignificant singular value truncation at the order of 2. That is, $\lambda_1 = \lambda_2 = 1$, and $0 \le \lambda_3 < 1$, then $\nu(d_2)$ is

$$\nu(d_2) = \frac{(u_{i1}^2 + u_{i2}^2 + \lambda_3 u_{i3}^2)^2}{u_{i1}^2 + u_{i2}^2 + \lambda_3^2 u_{i3}^2 + \sigma_w^2\left(\frac{1}{\sigma_1^2} + \frac{1}{\sigma_2^2} + \frac{\lambda_3^2}{\sigma_3^2}\right)}.$$

Letting A_0, B_0, C_0, and D_0 denote the nonnegative constants $u_{i1}^2 + u_{i2}^2$, u_{i3}^2, $\sigma_w^2(1/\sigma_1^2 + 1/\sigma_2^2)$, and $\sigma_w^2(\lambda_3^2/\sigma_3^2)$, respectively, $\nu(d_2)$ is simply represented as

$$\nu(d_2) = \frac{(A_0 + B_0\lambda_3)^2}{(A_0 + C_0) + (B_0 + D_0)\lambda_3^2}.$$

By letting the partial derivative of $\nu(d_2)$ with respect to λ_3 be zero, it is known that $\nu(d_2)$ takes a maximum value $\nu_{\max}(d_2) = (A_0^2(B_0 + D_0) + B_0^2(A_0 + C_0))/((A_0 + C_0)(B_0 + D_0))$ at $\lambda_{30} = B_0(A_0 + C_0)/(A_0(B_0 + D_0))$, $(0 < \lambda_{30} < 1)$ as illustrated in Fig. 2. When the sharp truncation of the ordinary rank reduction is used ($\lambda_3 = 0$), $\nu(d_2)$ is equal to $A_0^2/(A_0 + C_0)$. When the rank reduction is not used ($\lambda_3 = 1$), $\nu(d_2)$ is equal to $(A_0 + B_0)^2/(A_0 + B_0 + C_0 + D_0)$. Both values of $\nu(d_2)$ are, of course, less than the maximum value $\nu_{\max}(d_2)$. From the above simple example, if proper values are selected for a tapering window, it is obvious that rank reduction using a tapering window suppresses the ripple due to the low-order sharp truncation and clarifies the location of each excitation pulse. It is, however, difficult to select optimum values $\{\lambda_i\}$ of the tapering window. We describe two approaches to design the tapering window below.

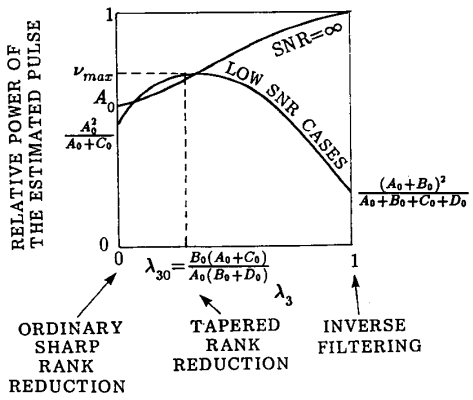

Fig. 2. The relative power of the estimated amplitude of the pulse to the total signal power. The tapered rank reduction simultaneously suppresses the noise term and the ripple which is caused by the sharp rank reduction and then clarifies the pulse locations.

A. Convolution by a Window Function

Let $[\delta_1, \delta_2, \cdots, \delta_N]$ denote the diagonal component of the matrix Δ_R of (11) obtained by ordinary rank reduction. By calculating the circular convolution between a $(2N - 2)$-length sequence of $[\delta_1, \delta_2, \cdots, \delta_{N-1}, \delta_N, \delta_{N-1}, \cdots, \delta_2, \delta_1]$ with a window function of $w(n)$, a $(2N - 2)$-length sequence of $[\lambda_1, \lambda_2, \cdots, \lambda_{2N-2}]$ is obtained. By selecting the first N elements of the sequence and using them, the $N \times N$ diagonal matrix $\Lambda = \text{diag}\,[\lambda_1, \lambda_2, \cdots, \lambda_N]$ is obtained. Then the minimum-norm least square estimate $\hat{x}$ is obtained using (12) or (13). For example, the $(2N_w + 1)$-length window function $w(n)$ is defined by the following Hamming window [33]:

$$w_H(n) = 0.54 + 0.46\cos(2\pi n/2N_w) \cdot (-N_w \le n \le N_w). \quad (16)$$

B. Minimization of Mean-Square Error

The response of the low-order-passing filter $U\Delta_R U^T$ of (11) to the impulse

$$d_i = [\overbrace{0, \cdots, 0}^{i-1}, 1, \overbrace{0, \cdots, 0}^{N-i}]^T$$

is $U\Delta_R U^T d_i$, which has a large ripple around the ith impulse. In order to suppress the ripple, the response is multiplied by an $N \times N$ weighting diagonal matrix, denoted by W_i, and the suppressed sequence f_i is given by

$$f_i = W_i U\Delta_R U^T d_i.$$

For each i, ($i = 1, 2, \cdots, N$), the desired response f_i to the impulse d_i is prepared using the weighting matrix W_i in advance. Since the characteristics of the W_i depend on the pulse location i, we cannot use the W_i to estimate multipulse input time series in practical cases. Thus, we determine an $N \times N$ diagonal matrix $\Lambda = \text{diag}\,[\lambda_1, \lambda_2, \cdots, \lambda_N]$ of (12) or (13) below.

Let an N-dimensional vector s_i denote the response sequence of the filter $U\Lambda U^T$ to d_i. That is

$$s_i = U\Lambda U^T d_i.$$

To determine the diagonal elements $\{\lambda_i\}$ of Λ, the following mean-square error α, which is defined by the difference between the desired response f_i and the response s_i of the filter $U\Lambda U^T$ to d_i, is minimized as

$$\alpha = \sum_{i=1}^{N} \| f_i - s_i \|^2$$

$$= \sum_{i=1}^{N} \| f_i - U\Lambda U^T d_i \|^2 \rightarrow \text{MIN}.$$

Since U is the unitary matrix

$$\alpha = \sum_{i=1}^{N} \| U^T f_i - \Lambda U^T d_i \|^2. \tag{17}$$

Using the ith column eigenvector $u_i = [u_{1i}, u_{2i}, \cdots, u_{Ni}]^T$ of U, the second term $\Lambda U^T d_i$ is equal to $U_i \vec{\lambda}$, where $U_i \overset{\text{def}}{=} \text{diag}\,[u_{i1}, u_{i2}, \cdots, u_{iN}]$ is an $N \times N$ matrix and $\vec{\lambda} \overset{\text{def}}{=} [\lambda_1, \lambda_2, \cdots, \lambda_N]^T$ is an N-dimensional vector. Using the property: $U_1^2 + U_2^2 + \cdots + U_N^2 = I$, α of (17) is arranged as

$$\alpha = \sum_{i=1}^{N} \| U^T f_i - U_i \vec{\lambda} \|^2$$

$$= \sum_{i=1}^{N} f_i^T f_i - 2 \sum_{i=1}^{N} f_i^T U U_i \vec{\lambda} + \vec{\lambda}^T \vec{\lambda}.$$

By taking the partial derivatives of α with respect to $\vec{\lambda}$ and setting the derivatives equal to zero, the coefficient vector $\vec{\lambda}$ of the tapering window is determined as

$$\vec{\lambda} = \sum_{i=1}^{N} (U_i U^T) f_i$$

$$= \sum_{i=1}^{N} (U_i U^T W_i U \Delta_R U^T)\, d_i. \tag{18}$$

Using the components $\{\lambda_i\}$ of the resultant vector $\vec{\lambda}$, the multipulse time series x is estimated from (12) or (13). For example, if the N-length Fourier transform of the Hamming window $w_H(n)$ of (16), denoted by $W_H(k)$, $(k = -N/2 + 1, \cdots, -1, 0, 1, \cdots, N/2)$, is used, the diagonal components of the weighting matrix $W_i = \text{diag}\,[W_{i1}, W_{i2}, \cdots, W_{iN}]$ to suppress the ripple around ith impulse are determined as $W_{ij} = W_H(j - i + 1)$.

By using the tapering window designed from either of these two methods, the ripple around each pulse location is suppressed.

IV. Determination of Pulse Locations by Pole Estimation

Using the multipulse time series $\hat{x}(n)$ estimated by the tapered rank reduction method, we propose an approach to accurately determine the pulse locations of the multipulse input time series $x(n)$ as follows:

Let $s(k)$ denote the inverse Fourier transform of the multipulse time series $\hat{x}(n)$ estimated above as

$$s(k) = \sum_{n=0}^{N-1} \hat{x}(n) \exp(j2\pi nk/N). \tag{19a}$$

If the sequence $\hat{x}(n)$ is ideally expressed by (1), then

$$s(k) = \sum_{i=1}^{N_p} d_i \cdot \exp(j2\pi\tau_i k/N). \tag{19b}$$

Thus, the inverse Fourier transform $s(k)$ of the estimated series $\hat{x}(n)$ is the sum of N_p complex sinusoids $d_i \exp(j2\pi\tau_i k/N)$. The frequency τ_i and the amplitude d_i of the ith sinusoid correspond, respectively, to the location and the amplitude of the ith pulse. In general, a deterministic process consisting of N_p complex sinusoids is represented by the N_pth order difference equation of the form [14]:

$$s(k) = -\sum_{i=1}^{N_p} b_i \cdot s(k - i) \tag{20}$$

where $\{b_i\}$ are coefficients of the polynomial:

$$B(z) = \sum_{i=0}^{N_p} b_i \cdot z^{-i} \qquad (b_0 = 1)$$

$$= \prod_{i=1}^{N_p} (1 - \beta_i \cdot z^{-1}). \tag{21}$$

By applying the high-resolution technique such as the MFBLP method [23]–[25], the coefficients $\{b_i\}$ are estimated as follows: Using an L-dimensional vector $\boldsymbol{b} = [b_1, b_2, \cdots, b_L]^T$ formed by the L weights $\{b_i\}$, $(L \geq N_p)$, the forward prediction error $e_f(k)$ and the backward prediction error $e_b(k)$ are, respectively, expressed as

$$e_f(k) = s(k) + \boldsymbol{s}_f(k)^T \boldsymbol{b} \tag{22a}$$

$$e_b(k) = s(k - L) + \boldsymbol{s}_b(k)^T \boldsymbol{b}^* \tag{22b}$$

where $\boldsymbol{s}_f(k)$ is the L-dimensional vector $[s(k-1), s(k-2), \cdots, s(k-L)]^T$, $\boldsymbol{s}_b(k)$ is the time-reversed L-dimensional vector $[s(k-L+1), \cdots, s(k-1), s(k)]^T$, and $*$ denotes the complex conjugate. The permissible upper limit of values for the predictor order L is equal to $N - N_p/2$ [25].

If the above model exactly represents the multipulse time series, both error terms, $e_f(k)$ and $e_b(k)$, are equal to zero for the period $k = L, L+1, \cdots, N-1$. Therefore, the coefficients $\{b_i\}$ are determined by minimizing the following squared error ϵ:

$$\epsilon = \sum_{k=L}^{N-1} \left\{ |e_f(k)|^2 + |e_b(k)|^2 \right\}. \rightarrow \text{MIN}. \tag{23a}$$

Let $\boldsymbol{s}$ be a $2(N-L)$-dimensional vector defined by $[s(L), s(L+1), \cdots, s(N-1), s^*(0), s^*(1), \cdots, s^*(N-L-1)]^T$, and let S be a $2(N-L) \times L$ matrix defined by $[\boldsymbol{s}_f(L), \boldsymbol{s}_f(L+1), \cdots, \boldsymbol{s}_f(N-1), \boldsymbol{s}_b^*(L), \boldsymbol{s}_b^*(L+1), \cdots, \boldsymbol{s}_b^*(N-1)]^T$. Using the matrix notation, the prediction error energy ϵ of (23a) is given by

$$\epsilon = (\boldsymbol{s} + S\boldsymbol{b})^H (\boldsymbol{s} + S\boldsymbol{b}), \rightarrow \text{MIN} \tag{23b}$$

where the superscript H denotes Hermite transpose. By minimizing ϵ with respect to $\boldsymbol{b}$, the deterministic normal equation is obtained as

$$S^H S\boldsymbol{b} = -S^H \boldsymbol{s}.$$

When the number of pulses is equal to N_p, the rank of the matrix S is equal to N_p. Thus, by using the SVD of S, a truncated SVD solution is obtained by setting the nonsignificant singular values

of S to zero. That is, the estimate $\hat{\boldsymbol{b}}$ of $\boldsymbol{b}$ is given by

$$\hat{\boldsymbol{b}} = -P_2\Gamma_{N_p}^{-1}P_1^H\boldsymbol{s} \tag{24}$$

where P_1 and P_2 are $2(N-L)\times 2(N-L)$ and $L\times L$ unitary matrices, respectively, and a $2(N-L)\times L$ diagonal matrix Γ has the ith singular value γ_i of S in the i, i position and zeros elsewhere, where $(\gamma_1 \geq \gamma_2 \geq \cdots \geq \gamma_L)$. Since the rank of S is N_p, $\gamma_{N_p+1} = \gamma_{N_p+2} = \cdots = \gamma_L = 0$ and the $L\times 2(N-L)$ inverse matrix $\Gamma_{N_p}^{-1}$ of Γ is defined by diag $[1/\gamma_1, 1/\gamma_2, \cdots, 1/\gamma_{N_p}, 0, \cdots, 0]$.

Using the complex coefficients $\{b_i\}$ obtained from (24), the root of the polynomial $B(z) = 0$ of (21). That is, the L poles $\{\beta_i = \exp(j2\pi\tau_i/N)\}$ are determined. The N_p largest poles $\{\beta_i\}$ are selected and the corresponding pulse locations $\{\hat{\tau}_i\}$, $(i = 1, 2, \cdots, N_p)$ are obtained by

$$\hat{\tau}_i = N\left[\tan^{-1}(\operatorname{Im}\beta_i/\operatorname{Re}\beta_i)\right]/2\pi.$$

If each pulse location τ_i is assumed to be restricted to one of the discrete sampling points $(n = 0, 1, \cdots, N-1)$, the corresponding sinusoid $\exp(j2\pi\tau_i/N)$ is continuous between $k = n-1$ and $k = 0$. Then, the prediction errors of (22a) and (22b) are alternatively defined by the circular convolution as

$$e_f(k) = \sum_{i=0}^{L} b_i \cdot s(k - i \bmod N) \tag{25a}$$

and

$$e_b(k) = \sum_{i=0}^{L} b_i \cdot s^*(k + i - L \bmod N). \tag{25b}$$

Since the error terms are defined for the period $k = 0, 1, \cdots, N-1$ instead of the period $k = L, L+1, \cdots, N-1$ of (23a), $\boldsymbol{s}$ and S of (23b) are redefined by $2N$-dimensional vector and $2N\times L$ matrix, respectively. Thus, the estimate $\hat{\boldsymbol{b}}$ is obtained by a similar procedure as described in (24).

The complex sinusoids $s(k)$ obtained from the inverse Fourier transform of the multipulse time series $\hat{x}(n)$ estimated in (12) or (13) is multiplied by the characteristics of the tapering window function. Thus, the usage of the tapering window in the rank reduction is analogous to the multiplication of a window used in the ordinary autocorrelation method [1] in the linear predictive coding, and the estimated poles $\{\beta_i\}$ fall inside the unit circle. Using the input signal estimated from the *tapered* rank reduction, therefore, the pulse positions of the multipulse time series are stably determined. This is another merit of the tapered rank reduction method.

V. Maximum Likelihood Estimation

Since the ML estimation of the pulse locations has high nonlinearity, it is very time consuming to obtain global minimum without using suitable initial values. It is, however, possible to obtain more accurate estimates by using the pulse locations estimated above as the initial values for the nonlinear optimization. Using the matrix notation and (19a), the prediction error of (22a), denoted by a $(N-L)$-dimensional vector $\boldsymbol{e}$, is given by

$$\begin{aligned}\boldsymbol{e} &= BF^HA\boldsymbol{y}\\ &= BF^HA(\boldsymbol{h} + \boldsymbol{w})\end{aligned} \tag{26}$$

where B is the $(N-L)\times N$ matrix:

$$B = \begin{pmatrix} b_L & b_{L-1} & \cdots & b_1 & b_0 & \cdots & 0\\ \vdots & \ddots & \ddots & \ddots & \ddots & \ddots & \vdots\\ 0 & \cdots & b_L & b_{L-1} & \cdots & b_1 & b_0 \end{pmatrix}$$

and the m, n element of the $N\times N$ matrix F is the Fourier operator $\exp\{-j2\pi mn/N\}$, $(m, n = 0, 1, \cdots, N-1)$.

If the above matrices B and A exactly represent the pulse locations and the transfer system, respectively, every component of the first term $BF^HA\boldsymbol{h}$ is equal to zero and then only the second term $BF^HA\boldsymbol{w}$ remains. Letting the term BF^HA be denoted by $(N-L)\times N$ matrix G, $\boldsymbol{e}$ is represented by

$$\boldsymbol{e} = G\boldsymbol{w}.$$

Since the rank of the matrix B equals $N-L$, the rank of the matrix G is also $N-L$. Then, the additive noise $\boldsymbol{w}$ is given by

$$\begin{aligned}\boldsymbol{w} &= G^+\boldsymbol{e}\\ &= G^+G\boldsymbol{y}\end{aligned} \tag{27}$$

where G^+ is the Moore–Penrose pseudoinverse matrix [32] of G of rank $(N-L)$ represented by means of the SVD. The power $\eta(\{b_i\})$ of the observed noise is defined as

$$\begin{aligned}\eta(\{b_i\}) &= |\boldsymbol{w}|^2\\ &= |G^+G\boldsymbol{y}|^2 \rightarrow \text{MIN.}\end{aligned} \tag{28}$$

Both the pulse locations $\{\tau_i\}$ and the noise signal $\boldsymbol{w}$ are estimated by minimizing the power η with respect to the complex linear coefficients $\{b_i\}$. Though this optimization has high nonlinearity, the global minimum is achieved by using an ordinary nonlinear optimization technique such as the Marquardt method [34] using the estimates obtained in Sections III and IV as the initial values.

VI. Simulation Results

In order to illustrate the advantages of the three-stage method proposed in Sections III–V over the ordinary inverse filtering method or the SVD-based method in Section II, we choose the popular example of the fourth-order all-pole model used in the literature [35]. The values of the linear predictive coefficients are $a_0 = 1$, $a_1 = -2.7607$, $a_2 = 3.8106$, $a_3 = -2.6535$, and $a_4 = 0.9238$. Fig. 3(a) shows the characteristics of the all-pole model. This all-pole model has 4 poles, which are close to the unit circle on the z plane. Thus, the ratio of the minimum and the maximum singular value of the matrix H is very small (approximately 10^{-3}) as shown in Fig. 3(b). Each method is implemented on an IBM3081 (1 word = 32 bit) computer using double precision arithmetic.

First Example: Consider the two-pulse input series $x(n)$, where the pulse locations are $\tau_1 = 4$ and $\tau_2 = 14$ and respective amplitudes are $d_1 = 1$ and $d_2 = -1$. Figs. 4(a) and (b) show the $x(n)$ and the response $h(n)$ of the transfer system to $x(n)$, respectively. The total length of the synthesized signal $y(n) = h(n) + w(n)$ is 32 points (Fig. 4(c)) and the SNR is equal to 10 dB. Fig. 4(d) shows the moving average process $A\boldsymbol{w}$ of (6), which has an average amplitude equal to 11.0. Thus, the amplitude of the multipulse time series $x(n)$ is so small as to be a tenth of the average amplitude of the noise term $A\boldsymbol{w}$, though the SNR is 10 dB.

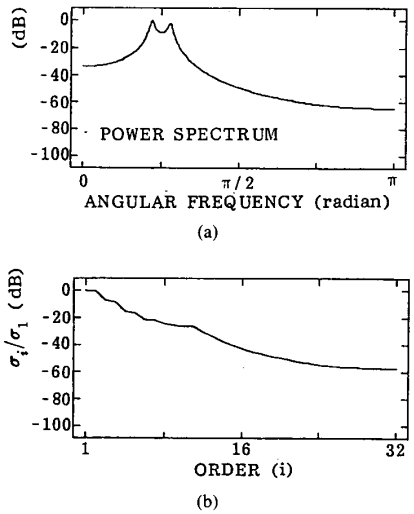

Fig. 3. (a) The power spectrum $1/|A(\omega)|^2$ of the all-pole model used in the experiments. (b) The singular values $\{\sigma_i\}$ of the matrix H.

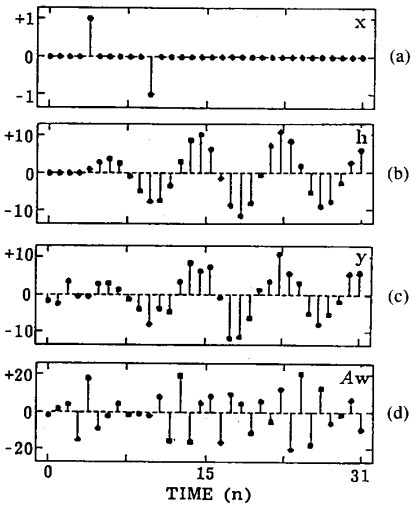

Fig. 4. (a) The 2-pulse input time series $x(n)$ for the first example. (b) The response $h(n)$ of the transfer system to $x(n)$. (c) The observed signal $y(n) = h(n) + w(n)$ (SNR = 10 dB). (d) The moving average process Aw.

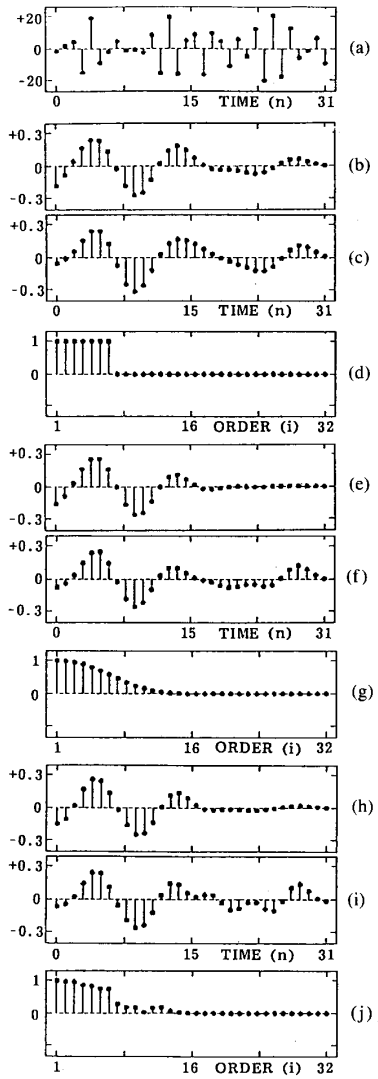

Fig. 5. Estimated multipulse time series. (a) The ordinary inverse filtering. (b) The ordinary rank reduction ($R = 10$), for SNR = ∞, (c) for SNR = 10 dB, (d) the diagonal components of the matrix Δ of (11) or Λ of (13). (e) The *tapered* rank reduction in Section III-A ($N_w = 8$), for SNR = ∞, (f) for SNR = 10 dB, (g) the diagonal components of the matrix Δ of (11) or Λ of (13). (h) The *tapered* rank reduction in Section III-B ($N_w = 2$), for SNR = ∞, (i) for SNR = 10 dB, (j) the diagonal components of the matrix Δ of (11) or Λ of (13).

Fig. 5(a) shows the multipulse time series estimated by the ordinary inverse filtering of (6). The resultant estimate is similar not to $x(n)$ but to the sequence Aw in Fig. 4(d). Figs. 5(b) and 5(c) show the multipulse time series obtained by using the ordinary rank reduction of (10) when the SNR equals ∞ and 10 dB, respectively. The truncation order R of (10) was determined by comparing the normalized ratio $\rho(R)$ [15, pp. 924–925]

$$\rho(R) = \sqrt{\frac{\sum_{i=1}^{R} |\delta_i|^2}{\sum_{i=1}^{N} |\delta_i|^2}} \tag{29}$$

with a threshold T_0. The R is equal to 7 when the T_0 is 99.7%. The characteristics of the diagonal components of the matrix Δ_R of (11) has low-order sharp truncation as shown in Fig. 5(d) and the sharp truncation leads to the large ripple (see also Fig. 1).

Figs. 5(e)–(g) and 5(h)–(j) show the multipulse time series estimated by the rank reduction using the tapering windows, each of which is designed by the method in Sections III-A and III-B, respectively. The width N_w of the tapering window is 8 in Fig. 5(e)–(g) and 2 in Fig. 5(h)–(j). Each diagonal component λ_i of Λ of (14) is shown in Fig. 5(g) and Fig. 5(j). The large ripple occurring around each pulse location in Fig. 4(b) is reduced in Figs. 5(e)–(g) and 5(h)–(j).

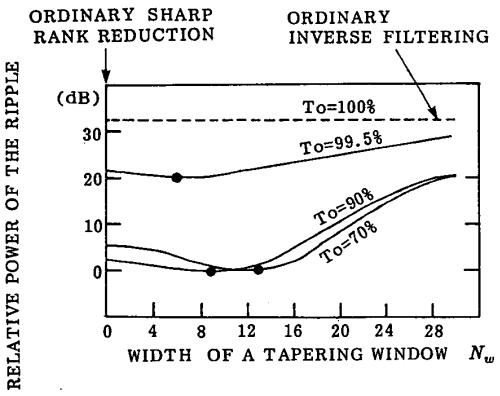

Fig. 6. The relative power ζ of the ripple caused around each original pulse location as a function of the width N_w of a tapering window and the threshold T_0 in (29). The minimum value is marked with "●."

Fig. 6 shows the normalized mean-square error ζ for various widths N_w of a tapering window, which is designed by the method in Section III-A. From the input series $\hat{x}(n)$ estimated in the case where the original time series $x(n)$ has only one impulse, that is, $x(n) = d_1\delta(n - \tau_1)$, the ζ is calculated as

$$\zeta = \frac{\sum_{n=0}^{N-1} \left|\hat{x}(n) - x'_\infty(n)\right|^2}{\sum_{n=0}^{N-1} \left|x'_\infty(n)\right|^2} \tag{30}$$

where

$$x'_\infty(n) = \begin{cases} x_\infty(n), & \tau_1 - N_B \le n \le \tau_1 + N_B; \\ 0, & \text{otherwise} \end{cases}$$

and $x_\infty(n)$ is the input time series estimated when SNR $= \infty$. By setting the value of N_B to be 1, ζ evaluates the relative power of the ripple caused around the original pulse location. In the figure, the value of ζ obtained for the case $N_w = 0$ indicates the relative power of the ripple of the input time series estimated by the ordinary sharp rank reduction. The minimum value of ζ is achieved by using a tapering window for each threshold T_0, and the minimum value of ζ is about 3 ~ 5 dB less than that obtained when the sharp rank reduction is used.

Fig. 7(a) shows the pulse locations estimated from the input time series in Fig. 5(f) using the proposed method in Section IV (SNR = 10 dB). The predictor order L used in (24) is equal to 4. Each of the estimated 4 poles $\{\hat{\beta}_i\}$ is marked with "×" in the z plane. The two largest roots are selected and the corresponding pulse locations $\hat{\tau}_i$ are shown by the mark "|" outside the unit circle. Fig. 7(b) shows the maximum likelihood estimates of the pulse locations based on the proposed method in Section V by using the estimates in Fig. 7(a) as the initial values. Figs. 7(b) and (c) show the estimates of the response of the all-pole model $h(n)$ and the multipulse time series $x(n)$, respectively, each of which agrees well with the original one in Fig. 4.

Second Example: In order to confirm the effect due to the tapering window, consider the three-pulse time series $x(n)$, where the pulse locations are $\tau_1 = 4$, $\tau_2 = 11$, and $\tau_3 = 14$ and the respective amplitudes are $d_1 = 1$, $d_2 = -1$, and $d_3 = -1$.

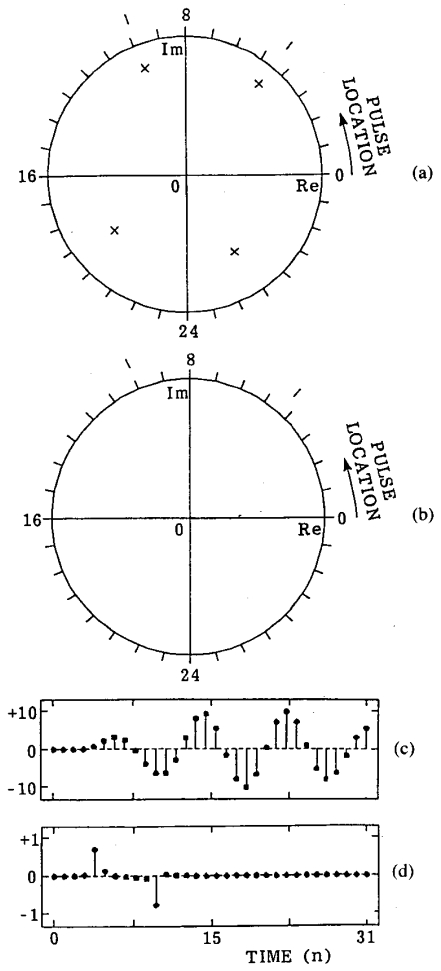

Fig. 7. (a) The pulse locations estimated from the sequence in Fig. 5(f) using the proposed method in Section IV (L = 18, SNR = 10 dB). (b) The maximum likelihood estimates in Section V using the pulse location estimates in Fig. 7(a) as the initial values, for the estimated pulse locations, (c) for the estimated response $h(n)$, and (d) for the estimated input time series $x(n)$.

The SNR of the synthesized signal $y(n)$, $(n = 0, 1, \cdots, 31)$ is equal to 15 dB.

Fig. 8(a) shows the poles $\{\hat{\beta}_i\}$, $(i = 1, 2, \cdots, L)$ and the pulse locations $\{\hat{\tau}_k\}$, $(k = 1, 2, 3)$ estimated in the 32 independent trials for various values of R. The width N_w and the predictor order L is equal to 8 and 12, respectively. Fig. 8(b) shows $\{\hat{\beta}_i\}$ and $\{\hat{\tau}_k\}$ for various values of N_w(R = 10 and L = 12). Fig. 8(c) shows $\{\hat{\beta}_i\}$ and $\{\hat{\tau}_k\}$ for various values of L(R = 10 and N_w = 8). These figures also show the average of the estimation error ϵ, which is defined by using the true pulse locations $\{\tau_i\}$ and their estimates $\{\hat{\tau}_i\}$ obtained from the above 32 independent trials as

$$\epsilon = E\left[\sqrt{\frac{1}{N_p}\sum_{i=1}^{N_p}\left|\tau_i - \hat{\tau}_i\right|^2}\right]. \tag{31}$$

The optimum values of R, N_w, and L are approximately equal to 10, 8, and 12, respectively. By comparing the results ob-

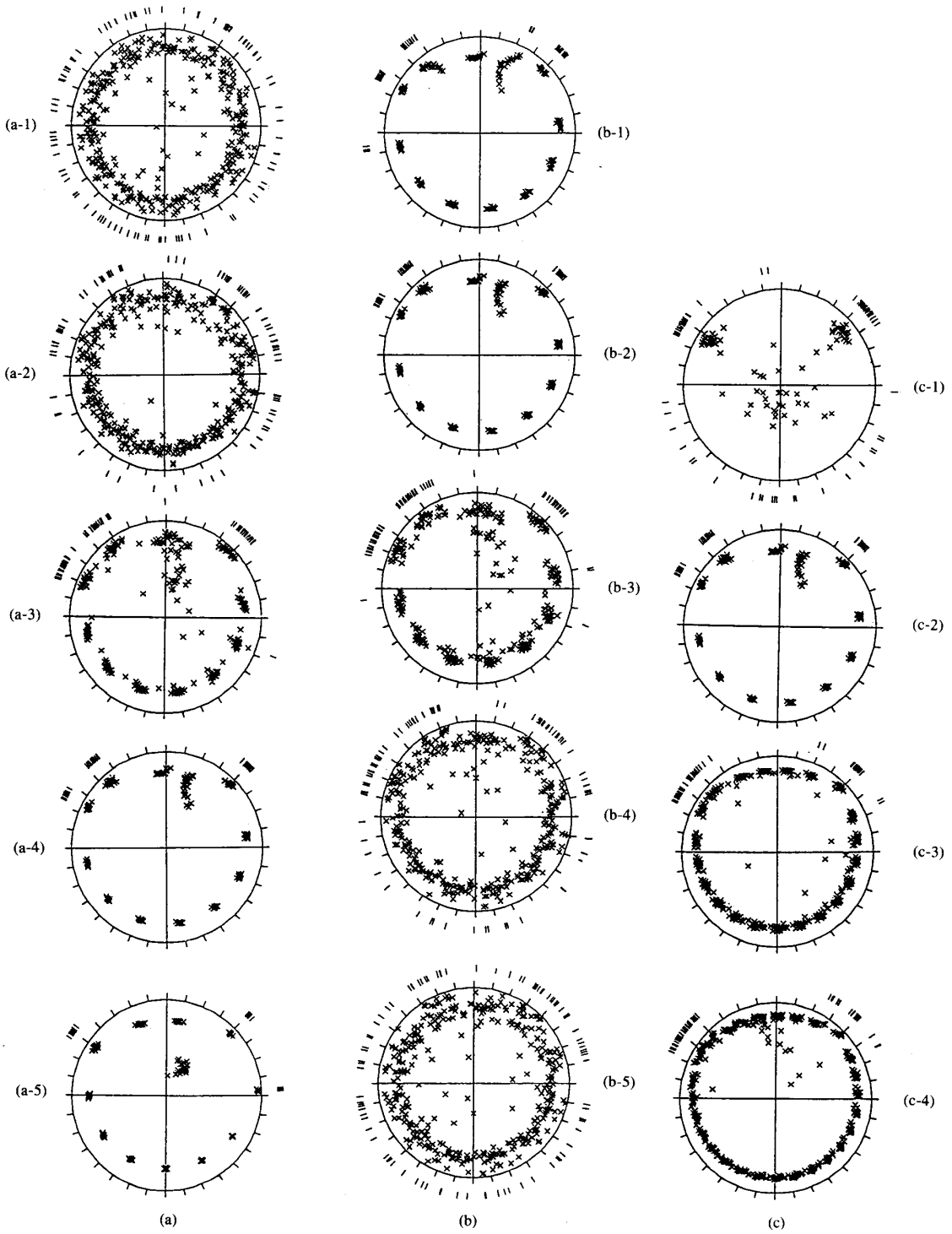

Fig. 8. The poles, marked by "×," and the pulse locations, marked by "|," estimated in the 32 independent trials for the second example (SNR = 15 dB) and the average values of the estimation error ϵ of (31). (a) For various values of the truncation order $R(N_w = 8, L = 12)$: (a-1) $R = 32$, inverse filtering, $\epsilon = 7.93$, (a-2) $R = 20$, $\epsilon = 6.99$, (a-3) $R = 14$, $\epsilon = 0.72$, (a-4) $R = 10$ (optimum) , $\epsilon = 0.45$, (a-5) $R = 5$, $\epsilon = 4.64$. (b) For various values of the width $N_w(R = 10, L = 12)$: (b-1) $N_w = 0$, ordinary sharp rank reduction, $\epsilon = 1.09$, (b-2) $N_w = 8$ (optimum), $\epsilon = 0.45$, (b-3) $N_w = 16$, $\epsilon = 1.05$, (b-4) $N_w = 24$, $\epsilon = 4.96$, (b-5) $N_w = 30$, $\epsilon = 6.53$. (c) For various values of the predictive order $L(R = 10, N_w = 8)$: (c-1) $L = 3$, $\epsilon = 5.07$, (c-2) $L = 12$ (optimum), $\epsilon = 0.45$, (c-3) $L = 21$, $\epsilon = 1.11$, (c-4) $L = 27$, $\epsilon = 1.56$.

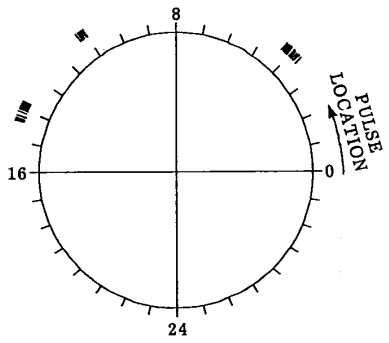

Fig. 9. The maximum likelihood estimates of the pulse locations using the proposed method in Section V for the 32 independent trials (SNR = 15 dB). The estimates in Fig. 8(a-4) are used as the initial values.

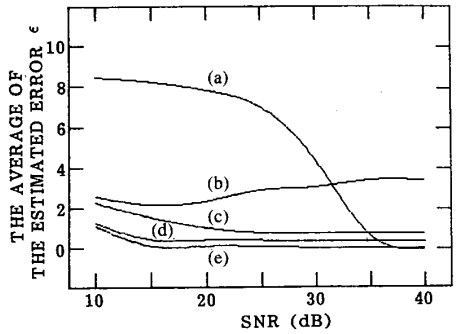

Fig. 10. The comparison of the pulse locations estimated by the five methods for various SNR for the second example. (*a*) The ordinary inverse filtering. (*b*) The ordinary rank reduction ($R = 10$). (*c*) The tapered rank reduction method in Section III-A ($N_w = 8$). (*d*) The pole-estimation method in Section IV ($L = 18$). (*e*) The maximum likelihood estimate in Section V.

tained by tapered rank reduction (Fig. 8(b-3), $\epsilon = 0.45$) with those obtained by the inverse filtering (Fig. 8(a-1), $\epsilon = 7.93$) and the ordinary sharp rank reduction (Fig. 8(b-1), $\epsilon = 1.09$), it is obvious that the usage of the tapering window increases the estimation accuracy.

The average of the residual power η of (28) is about 21.4 for the initial estimates obtained from the method in section 4 ($R = 10$, $N_w = 8$, and $L = 12$) with regard to the above 32 independent trials. By applying the ML estimation proposed in Section V to the results obtained from the above 32 independent trials, the average of the η was reduced to about 5.88, where the true value of the noise power σ_w^2 is equal to 5.97. The average value of the error ϵ of (31) for the estimated pulse locations, which are refined as shown in Fig. 9, is considerably reduced to 0.143.

Fig. 10 shows the average of ϵ of (31) concerning the 32 trials as a function of SNR. For the inverse filtering (*a*), the ordinary sharp rank reduction (*b*), and the tapered rank reduction (*c*), the pulse locations $\{\hat{\tau}_i\}$ are calculated from the locations corresponding to the three maximum amplitudes of the absolute values of the estimated input time series. From the figure, each of the proposed three methods is obviously effective even in low SNR cases.

Third Example: Consider the following seven-pulse time series $x(n)$ as shown in Fig. 11(a). The SNR is equal to 18 dB. Figs. 11(b) and 11(c) show the estimates of the multipulse time

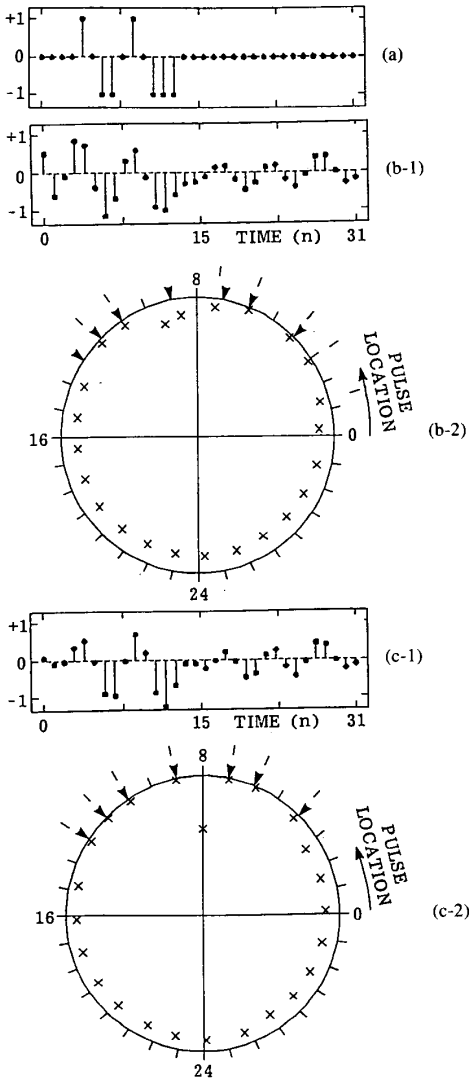

Fig. 11. The results of the simulation experiments for the third example. (a) The original 7-pulse time series $x(n)$. (b) The ordinary sharp rank reduction ($R = 10$). (c) The tapered rank reduction in Section III-A ($N_w = 4$). (b-2) and (c-2) show the pulse locations estimated from the sequences in (b-1) and (c-1), respectively. Each of true pulse locations is marked with "▼."

series and the pulse locations. There are some errors in the pulse locations of Fig. 11(b-2), which is estimated when the pole-estimation method proposed in Section IV is applied to the multipulse time series in Fig. 11(b-1) obtained by the ordinary sharp rank reduction ($N_w = 0$). However, when the pole-estimation method is applied to the multipulse input time series in Fig. 11(c-1) obtained from the tapered rank reduction method ($N_w = 8$, $R = 10$, and $L = 18$), the satisfactory result is obtained as shown in Fig. 11(c-2).

VII. Concluding Remarks

In order to estimate the multipulse time series from the response of the all-pole transfer system in the case where the system Q (quality factor) is high and the SNR is low, the ML

estimation requires high nonlinear optimization and then it is important to select suitable initial estimates. On the other hand, for other methods such as the pole estimation method, it is necessary to remove the characteristics of the transfer system before determining each pulse location. In order to avoid these difficulties, we proposed an alternative three-stage method. The multipulse time series is estimated by the tapered rank reduction method. By applying the pole-estimation method to the inverse Fourier transform of the resultant multipulse series, the pulse locations are determined accurately. By using the pulse locations as the initial estimates, more accurate maximum likelihood estimates of the pulse locations are obtained. From the simulation experiments, these principles were confirmed.

In the experiments, the order M and the parameters $\{a_m\}$, $m = 1, 2, \cdots, M$ of the all-pole transfer system and the number N_p of pulses of the multipulse time series are already known. However, in general, it is difficult to choose these unknown parameters for an unknown signal. It is also important to choose the optimum values of the truncation order R, the width N_w of the tapering window, and the predictive order L, using the relation between the values of these parameters and the SNR. These important issues are currently under investigation. It is also important to apply the proposed procedure to some practical examples.

Acknowledgment

The authors would like to thank Prof. Dr. N. Chubachi, Dr. S. Makino, and Dr. Y. Kawazoe at Tohoku University and Dr. H. Suzuki at Ono Sokki Co., Ltd.

References

[1] J. D. Markel and A. H. Gray, Jr., *Linear Prediction of Speech.* Berlin, Heidelberg: Springer, 1976.

[2] B. S. Atal and J. R. Remde, "A new model of LPC excitation for producing natural sounding speech at low bit rates," presented at the IEEE Int. Conf. Acoust., Speech, Signal Processing, pap. S5.10, May 1982.

[3] G. C. Carter, Ed., *IEEE Trans. Acoust., Speech, Signal Processing* (Special Issue on Time Delay Estimation), vol. ASSP-29, no. 3, June 1981.

[4] M. T. Silvia, *Handbook of Digital Signal Processing Engineering Applications*, D. F. Elliot, Ed. New York: Academic, 1987, ch. 10, 11.

[5] J. E. Ehrenberg, T. E. Ewatt, and R. D. Morris, "Signal processing techniques for resolving individual pulses in multipath signal," *J. Acoust. Soc. Amer.*, vol. 63, no. 6, pp. 1861–1865, June 1978.

[6] R. J. P. DeFigueiredo and C.-L. Hu, "Waveform feature extraction based on Tauberian approximation," *IEEE Trans. Pattern Analysis Mach. Intel.*, vol. PAMI-4, pp. 105–116, Mar. 1982.

[7] J. P. Ianniello, "Lower bounds on worst case probability of large error for two channel time delay estimation," *IEEE Trans. Acoust., Speech, Signal Processing*, vol. ASSP-33, no. 5, pp. 1102–1110, Oct. 1985.

[8] J. P. Ianniello, "Large and small error performance limits for multipath time delay estimation," *IEEE Trans. Acoust., Speech, Signal Processing*, vol. ASSP-34, no. 2, pp. 245–251, Apr. 1986.

[9] J. P. Ianniello, "High-resolution multipath time delay estimation for broad-band random signal," *IEEE Trans. Acoust., Speech, Signal Processing*, vol. ASSP-36, no. 3, pp. 320–327, Mar. 1988.

[10] J. P. Ianniello, "Time delay estimation via cross correlation in the presence of large estimation errors," *IEEE Trans. Acoust., Speech, Signal Processing*, vol. ASSP-30, pp. 988–1003, 1982.

[11] M. A. Pallas, N. Martin, and J. Martin, "Time delay estimation by autoregressive modelization," in *Proc. IEEE Int. Conf. Acoust., Speech, Signal Processing*, 1987, pp. 12.6.1–12.6.4.

[12] R. J. Tremblay, G. C. Carter, and D. W. Lytle, "A practical approach to the estimation of amplitude and time delay parameters of a composite signal in nonwhite Gaussian noise," in *Proc. IEEE Int. Conf. Acoust., Speech, Signal Processing*, 1987, pp. 12.9.1–12.9.4.

[13] R. J. P. DeFigueiredo and A. Gerber, "Separation of superimposed signals by a cross-correlation method," *IEEE Trans. Acoust., Speech, Signal Processing*, vol. ASSP-31, no. 5, pp. 1084–1089, Oct. 1983.

[14] S. M. Kay and S. L. Marple, Jr., "Spectral analysis—a modern perspective," *Proc. IEEE*, vol. 69, no. 11, pp. 1380–1419, Nov. 1981.

[15] J. A. Cadzow, "Spectral estimation: An overdetermined rational model equation approach," *Proc. IEEE*, vol. 70, no. 9, pp. 907–939, Sept. 1982.

[16] G. E. P. Box and G. M. Jenkins, *Time Series Analysis Forecast and Control.* Oakland, CA: Holden-Day, 1976.

[17] B. Friedlander and B. Porat, "A spectral matching technique for ARMA parameter estimation," *IEEE Trans. Acoust., Speech, Signal Processing*, vol. ASSP-32, no. 2, pp. 338–343, Apr. 1984.

[18] C. H. Knapp and G. C. Carter, "The generalized correlation method for estimation of time delay," *IEEE Trans. Acoust., Speech, Signal Processing*, vol. ASSP-24, pp. 320–327, Aug. 1976.

[19] B. M. Bell and T. E. Ewart, "Separating multipaths by global optimization of a multidimensional matched filter," *IEEE Trans. Acoust., Speech, Signal Processing*, vol. ASSP-34, no. 5, pp. 1029–1037, Oct. 1986.

[20] I. P. Kirsteins, "High resolutions time delay estimation," in *Proc. IEEE Int. Conf. Acoust., Speech, Signal Processing*, 1987, pp. 12.5.1–12.5.4.

[21] Z. Hou and Z. Wu, "A new method for high-resolution estimation of time delay," in *Proc. IEEE Int. Conf. Acoust., Speech, Signal Processing* (Paris), May 1982, pp. 420–423.

[22] Y. T. Chan, J. G. Bryan, and G. A. Lampropoulos, "Determining time delay via frequency estimation," in *Proc. IEEE Int. Conf. Acoust., Speech, Signal Processing* (Tokyo), Apr. 1986, pp. 2803–2806.

[23] D. W. Tufts and R. Kumaresan, "Estimation of frequencies of multiple sinusoids: Making linear prediction perform like maximum likelihood," *Proc. IEEE*, vol. 70, pp. 975–989, Sept. 1982.

[24] R. Kumaresan and D. W. Tufts, "Estimating the parameters of exponentially damped sinusoids and pole-zero modeling in noise," *IEEE Trans. Acoust., Speech, Signal Processing*, vol. ASSP-30, no. 6, pp. 833–840, Dec. 1982.

[25] R. Kumaresan, "On the zeros of the linear prediction error filter for deterministic signals," *IEEE Trans. Acoust., Speech, Signal Processing*, vol. ASSP-31, pp. 217–220, 1983.

[26] B. Porat and B. Friedlander, "On the accuracy of the Kumaresan-Tufts method for estimating complex damped exponentials," *IEEE Trans. Acoust., Speech, Signal Processing*, vol. ASSP-35, no. 2, pp. 231–235, Feb. 1987.

[27] T. L. Henderson, "Geometric methods for determining system poles from transient response," *IEEE Trans. Acoust., Speech, Signal Processing*, vol. ASSP-29, no. 5, pp. 982–988, Oct. 1981.

[28] K. Konstantinides and K. Yao, "Statistical analysis of effective singular values in matrix rank determination," *IEEE Trans. Acoust., Speech, Signal Processing*, vol. ASSP-36, no. 5, pp. 757–763, May 1988.

[29] L. L. Scharf and D. W. Tufts, "Rank reduction for modeling stationary signals," *IEEE Trans. Acoust., Speech, Signal Processing*, vol. ASSP-35, no. 3, pp. 350–355, Mar. 1987.

[30] H. Kanai and K. Kido, "Estimation of multipulse series driving of an all-pole transfer system," *Trans. Japan. Soc. Mech. Eng.*, vol. 54, ser. C, pp. 2907–2914, 1988 (in Japanese).

[31] M. Wax and T. Kailath, "Detection of signals by information theoretic criteria," *IEEE Trans. Acoust., Speech, Signal Processing*, vol. ASSP-33, no. 2, pp. 387–392, Apr. 1985.

[32] P. Lancaster and M. Tismenetsky, *The Theory of Matrices.* Academic, 1985.

[33] A. V. Oppenheim and R. W. Schafer, *Digital Signal Processing.* Englewood Cliffs, NJ: Prentice-Hall, 1975.

[34] S. L. Jacoby, J. S. Kowalik, and J. T. Pizzo, *Iterative Methods for Nonlinear Optimization Problem.* Englewood Cliffs, NJ: Prentice-Hall, 1972.

[35] A. H. Nutall, "Spectrum analysis of a univariate process with bad data points, via maximum entropy and linear predictive techniques," NUSC Sci. Eng. Studies, Spectral Estimation, Naval Underwater Syst. Center, New London, CT, Tech. Rep. 5303, Mar. 26, 1976.

Hiroshi Kanai (A'88) was born in Matsumoto, Japan, on November 29, 1958. He received the B.E. degree from Tohoku University, Sendai, Japan, in 1981, and the M.E. and the Dr. Eng. degrees, also from Tohoku University, in 1983 and in 1986, respectively, both in electrical engineering.

From 1986 to 1988 he was with the Education Center for Information Processing, Tohoku University, as a Research Associate. In 1989 he joined the Faculty of Engineering, Tohoku University, and since 1990 he has been a Lecturer in the Department of Electrical Engineering. His present interest is in digital signal processing and its applications to acoustical, ultrasonic, and electrical measurements.

Dr. Kanai is member of the Acoustical Society of Japan, the Institute of Electronics, Information, and Communication Engineering of Japan, the Japan Society of Mechanical Engineers, the Japan Society of Ultrasonics in Medicine, and Japan Society of Medical Electronics and Biological Engineering.

Ken'iti Kido (M'75) was born in Hamhun, Korea, on April 15, 1926. He received the B. Eng. degree in electrical engineering and the Dr. Eng. degree in acoustics from Tohoku University, Sendai, Japan, in 1948 and 1962, respectively.

In 1948, he worked with the Research Institute of Electrical Communication, Tohoku University, as a Research Associate. In 1957 he was an Associate Professor in the Faculty of Engineering. In 1963 he was a Professor of Acoustics at the Research Institute of Electrical Communication, and since 1976 he has been a Professor of Information Science at the Research Center for Applied Information Sciences, Tohoku University, and the Director of the Center. His present research interest is in digital signal processing and its application to acoustics and speech recognition.

Dr. Kido is a Fellow of the Acoustical Society of America. From 1983 to 1985 he was President of the Acoustical Society of Japan.